

Surface Shape Measuring Method for Space Structures Based on Images in Ultra-Violet Range

By Naoko KISHIMOTO,¹⁾ Takashi IWASA,²⁾ and Ken HIGUCHI³⁾

¹⁾*Department of Mechanical Engineering, Setsunan University, Neyagawa, Japan*

²⁾*Tottori University, Tottori, Japan*

³⁾*Muroran Institute of Technology, Muroran, Japan*

(Received June 23rd, 2017)

We have worked to develop new optical surface shape measuring methods enable to grasp surface shape of large space structures with high precision and high speed on orbit for future space antenna and telescope. These methods are applicable to testing such structures on ground. In these methods, we analyze phase values of projected or painted grating patterns on the structures and perform calibration using a reference plane. It is hard to project such patterns on large structural surface on orbit, however, we must paint some grating patterns on the structures. In that case, high contrast images of grating patterns, for example white and black grating painting, are needed for precise measurement. Nevertheless, high contrast white and black patterns on surface make thermo-optical features of the structure more complex, then there is a possibility of interfering with thermal design of spacecraft. Therefore, to widen the application range of our method, we propose surface shape measuring method based on grating patterns using ultra-violet range. We use two different kinds of painting materials and cameras having sensitivity to light of ultra-violet range. Both painting materials are photographed as white in the visible range, however, one is white and one is black in the ultra-violet range. In this method, we can get high contrast grating images on the surface only in the ultra-violet range. In this study, we provide some feasibility study using commercially available ultra-violet cameras and painting materials such as titanium oxide.

Key Words: Surface Shape Measurement, Image Measuring Method, Ultra-Violet Range

1. Introduction

A large space structure capable of keeping its surface shapes in orbit is demanded in future advanced space engineering missions as well as space science missions.¹⁻⁵⁾ A large deployable space antenna intended for a radio astronomy electrical wave observation in a high frequency domain is an example of the precise large space structures. To construct such a precise space structure in an orbit, the required accuracy of the surface shape is hardly accomplished with the traditional passive design approaches, and an active shape control technique is necessary.^{2,5)} When the active shape control technique is applied to the space structures, a precise and a short time shape measurement method is required to determine an appropriate control output instantaneously. Such a high accurate shape measurement method is also necessary for validating the surface shapes when the precise large space structures are tested on the ground before launching. Accordingly, an establishment of the precise and short time whole field surface measurement method for the large space structures is a key issue in the future space structure engineering.

Measurement methods that we have worked on include a grating projection method using a projector, and an imparted grating pattern method⁶⁻⁸⁾ in which a two-dimensional grating pattern attached to the object surface without a projector. In either method, the phase of the obtained grating image is

analyzed and the three-dimensional shape of the surface is calculated. For the phase derivation, there are a phase shift method calculating from several grating images with phase shifted patterns and a sampling moiré method calculating from just one grating image. Moreover, we adopt calibration method using two reference planes free from a factor of distortion due to lens aberration of cameras and projectors. The measurement accuracy is mainly determined on the resolution of cameras and distance between two reference planes which is equivalent to measuring space in depth direction.

These measurement methods have several advantages that it would allow inexpensive and simple system using commercially available devices, fast shape calculation, and high measuring resolution in space. And we have developed mobile system aiming to mount on a satellite to measure surface shape of large space structures with high precision such as space antenna and radar panel. In case of measuring large space structures on orbit, there are several problems as follows. (1) It is difficult to prepare a reference plane having a large area with respect to a large structure over 10 m. (2) To realize high resolution in the depth direction, the measurement space becomes too small to deep uneven structures. (3) In case of grating projection method, it is difficult to project grating pattern on a large space structure on orbit. To solve first two problems, we have proposed integrating results obtained by

dividing the region. We also propose a method of using the measurement object itself as the reference plane for calibration. In these methods, a large reference plane is unnecessary.

To solve the last problem, we preferably adopt the imparted grating pattern method in which a two-dimensional grating pattern attached to the object surface without a projector. However, according to Ref. 9) the solar absorptances of 20 types of black coatings are 0.88 to 0.97, the emissivities at 300 K are 0.72 to 0.94, whereas the solar absorptances of 38 types of white coatings are 0.06 to 0.44, emissivities at 300 K are 0.82 - 0.92,⁹⁾ and the black-and-white grating pattern on the structure surface is likely to interfere with the thermal design of spacecrafts. Therefore, to whiden the application range of our method, we propose a measurement method using ultraviolet (UV) range in addition to the visible (VIS) range . Specifically, a grating pattern is imparted on the surface of the structure by reflection/absorption materials in UV range. This grating pattern, which is entirely seen with VIS light as white, is photographed as black-and-white using a camera sensitive to UV rays. In this paper, we show both images in VIS/UV range of grating pattern imparted by combining UV ray reflecting/absorbing materials. And we provide result of three-dimensional measurement experiment using two UV cameras, and evaluate its effectiveness and measurement accuracy.

2. Surface Shape Measurement Method Using Ultra-Violet Range

2.1. Outline of the proposed method

First, we briefly describe the grating projection and imparted grating pattern method we have worked on so far. The outline of the measurement method is shown in Fig. 1. A grating pattern projected or imparted on the surface of the object is photographed by one or two cameras, a phase of each pixel of an obtained image is calculated from a brightness value, and finally three-dimensional position information of each pixel is calculated so that high spatial resolution in three-dimensional data is realized. Calibration is carried out using two reference planes and a measurement space is constructed for a measurement system composed of a camera

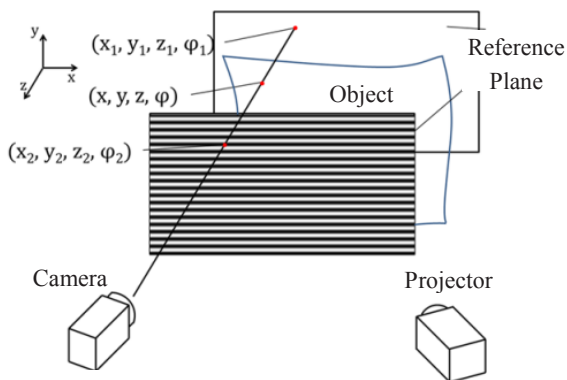


Fig. 1. Outline of grating projection method.

or a projector. This calibration allows free from distortion due to lens aberrations of cameras and projectors, and fast shape calculation. Since three-dimensional information can be obtained for each pixel of one image if using sampling Moiré method, analysis of a motion picture is also available.

2.2. Camera and painting material in ultra-violet range

In this research, 1.5 million pixel commercially available UV camera (Artley Co., Ltd., 407 UV-WOM, CCD monochrome image sensor, 1360 pixel×1024 pixel) was used. Two types of cameras depending on the presence or absence of a VIS light absorbing filter in front of the image sensor were prepared. Figure 2 shows the spectral sensitivity characteristics of the UV camera used in this study. A VIS light absorbing filter was not used. An UV transmission lens (Ricoh Imaging Corporation B 2528-UV), which center frequency is 365 nm, was also used.

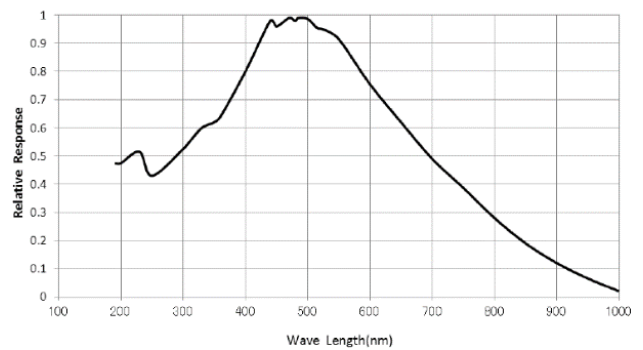


Fig. 2. Spectral characteristics of ultraviolet camera.¹⁰⁾

As ordinary fine paper has ultraviolet reflection characteristics, grating pattern was imparted on a sheet of fine paper using several painting materials with UV absorption characteristics. The UV absorbers used in this paper are listed in Table 1. We used four kinds of oxides as dispersed liquid. Commercial sunscreen cosmetic and UV-ray cut film include organic materials such as benzoic acid derivative, cinnamic acid derivative, and benzophenone derivative as UV absorber materials.

Table 1. Ultraviolet absorber.

UV absorber		remarks
Titanium oxide	HTD-710T	Particle dia. :15-50 nm
	ND134	Particle dia. :10-15 nm
Zinc oxide	HTD-711Z	Particle dia. :20-30 nm
Cerium oxide		Polishing material
Sunscreen cosmetic	Nivea	
	Anessa	
UV-ray cut film for window glass		

3. Feasibility Study for Proposed Method

3.1. Dynamic range of obtained images in UV range

Since three-dimensional information is derived from phase value calculated from brightness of each pixel captured grating pattern image, a dynamic range between white and black region in an obtained image directly effect on the measurement accuracy. A sample with prating pattern

imparted on fine paper with UV absorber was made and photographed with both ordinary camera in VIS and UV camera under indoor fluorescent light. Obtained images are shown in Fig. 3. In both images, the whole surface is white and dynamic range of grating pattern is small, since fluorescent lamp light contains almost no UV rays. Figure 4 shows grating images in UV range under UV LED lamp. A sufficient dynamic range is obtained.

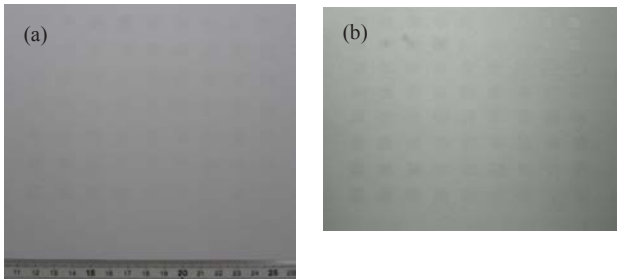


Fig. 3. Grating image under a fluorescent lamp indoors. (a) Image in VIS range. (b) Image in UV range.

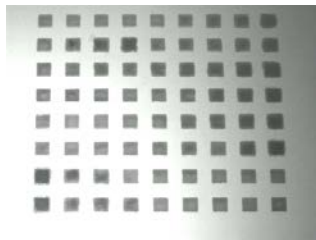


Fig. 4. Grating image in UV range under UV lamp.

Table 2 shows dynamic ranges expressed by brightness value of grating images in UV range. The value of most white part is set to 255, because the image is displayed in 8 bit gray scale. In other words, smaller value of most black part means larger dynamic range. Sufficient dynamic range is obtained with any UV absorbers, but a large dynamic range could be obtained particularly with titanium oxide or zinc oxide dispersed liquid. Therefore, titanium oxide was used as an UV absorber in the following measurement experiment.

Table 2. Dynamic ranges of grating images in UV range.

UV absorber		brightness value		
		white	black	
Titanium oxide	HTD-710T	255	50	
	ND134		40	
Zinc oxide	HTD-711Z		45	
Cerium oxide			80	
Sunscreen cosmetic	Nivea		96	
	Anessa		63	
UV-ray cut film for window glass				57

The optical features of titanium oxide are introduced here. Figure 5 shows spectral property of sunlight¹¹⁾ and spectral reflectivity of titanium oxide painting with particle size of 250nm.¹²⁾ It has high reflectivity over a wide wavelength range included in sunlight. Titanium oxide used in this study is presumed to have the same spectral properties, but because its particle size is relatively small, it is necessary to newly

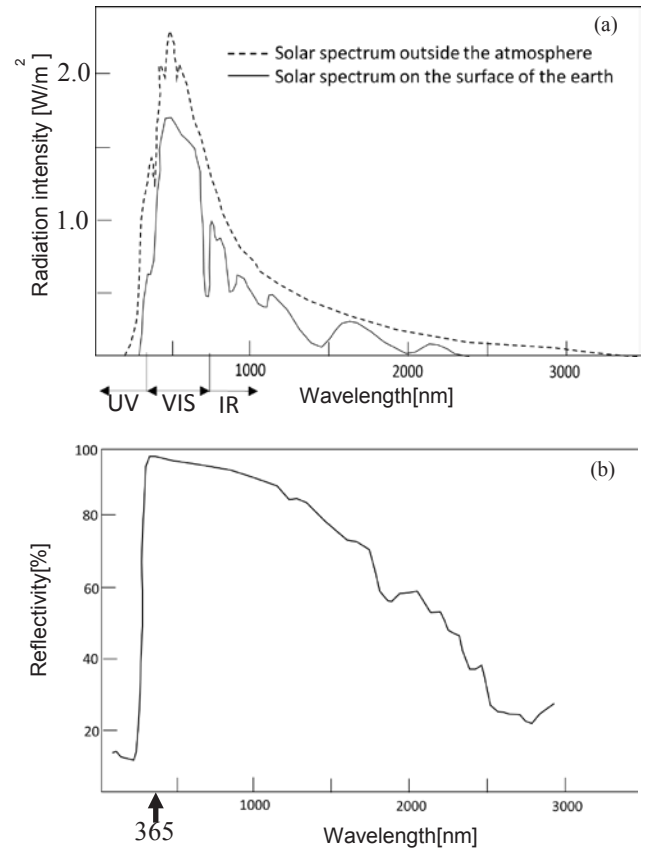


Fig. 5. Optical property of sunlight and titanium oxide painting. (a) Spectram property of sunlight. (b) Spectram reflectivity of titanium oxide paintings.

measure accurate spectral reflection characteristics. In addition, according to Ref. 10) two types of titanium oxide white paints, with Methyl Silicone and with Potassium Silicate, have solar absorptance of 0.20 and 0.17, emissivity at 300 K of 0.90 and 0.92, respectively.

3.2. UV intensity and dynamic range

In order to confirm whether sufficient dynamic range can be obtained with the amount of UV light contained in sunlight, we conducted experiments with varying UV intensity. For UV intensity measurement, an UV light meter (Lutron UV-340A) capable of measuring UV intensity of wavelength from 290 nm to 390 nm was used. Prior to the experiment, UV intensity was measured outdoors in fine weather (September 15, 2017), and it was about 2000 $\mu\text{W}/\text{cm}^2$ in the sun and about 250 $\mu\text{W}/\text{cm}^2$ in the shade. The UV intensity was varied by changing the distance from the UV lamp to the grating pattern sample shown in Fig. 3. The photographing conditions were set to 247 for the global gain and 1/8 for the shutter speed. Figure 6 shows grating images at different UV intensity and Fig. 7 shows grayscale value of grating images at different UV intensity. In the case of this photographing condition, when the UV intensity becomes 50 $\mu\text{W}/\text{cm}^2$ or less, it is difficult to distinguish the grating pattern. Since it is over 200 $\mu\text{W}/\text{cm}^2$ in the shade of fine weather, it is sufficient UV intensity to discriminate the grating pattern.

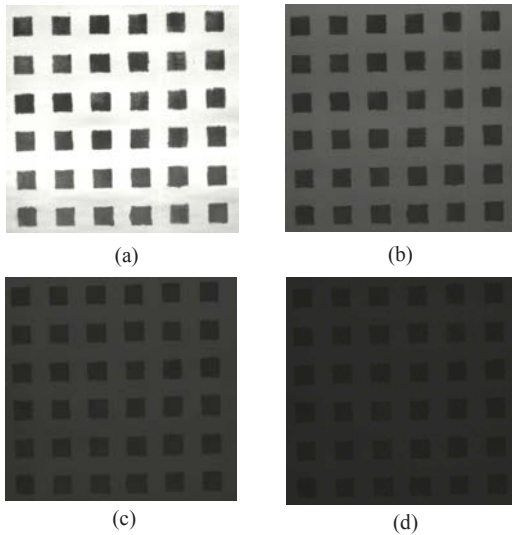


Fig. 6. Grating image at different UV intensity. (a) $340 \mu\text{W}/\text{cm}^2$, (b) $103 \mu\text{W}/\text{cm}^2$, (c) $52 \mu\text{W}/\text{cm}^2$, (d) $25 \mu\text{W}/\text{cm}^2$.

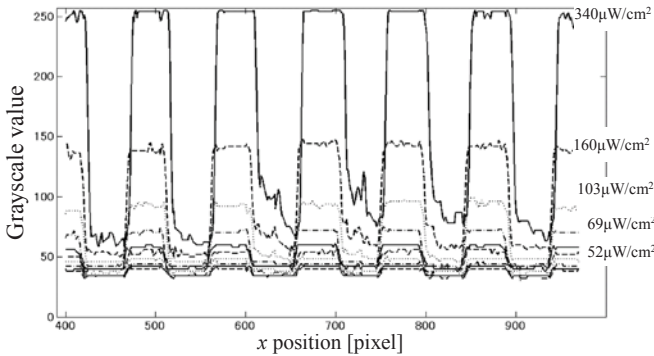


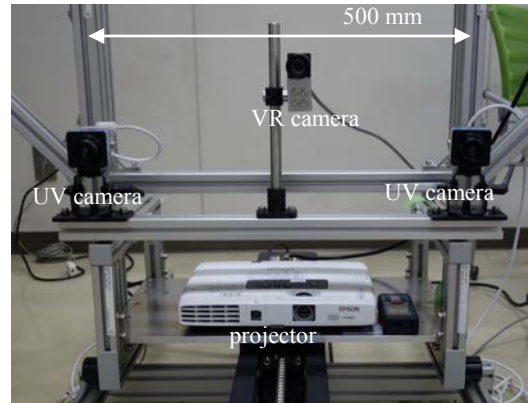
Fig. 7. Grayscale value of grating images.

3.3. Measuring experiment in UV range

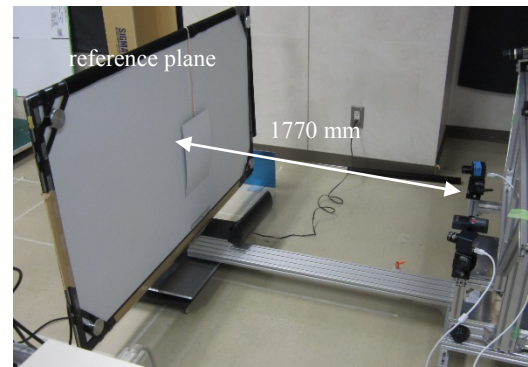
We conducted measurement experiment using the object imparted with a grating pattern using titanium oxide dispersion liquid with two UV cameras. In order to evaluate its effectiveness and accuracy, we also measured the same object by grating projection method. Measuring set up is shown in Fig. 8. The distance between two UV cameras is 500 mm. Figure 8(b) shows the reference plane, which is 60-inch plasma display, 1770 mm away from camera and projector. Specifications of measurement equipment including camera and projector are shown in Table 3.

Table 3. Specification of measurement equipment.

VIS camera	UI-3580CP×1 (iDS, 2560×1920 pixels)
UV camera	407 UV-WOM×2 (Artray, 1360×1024 pixels)
Projector	EB-1771W (EPSON, 1280×800 pixels)
Reference plane	60-inch Plasma Display (Panasonic, 1920×1080 pixels)
Linear slider	SGSP46-500 (SIGMAKOKI, positioning accuracy: 6 μm)
UV LED light	NCSU276AT/U365 (NICHIA, 365 nm)



(a)



(b)

Fig. 8. Measurement experiment set up. (a) Camera and projector. (b) Reference plane.

As the object to be measured, a cylindrical trash box (diameter about 200 mm, height about 300 mm) with fine paper imparted with grating pattern drawn by titanium oxide was used (Fig. 9). The grating pattern pitch is 8 mm.



Fig. 9. Trash box with grating pattern.

First, a two-dimensional cosine grating pattern with a pitch of 9 mm was displayed on the reference plane monitor, and calibration was performed with the reference plane distance set to 30 mm. It is possible to calibrate with the two-dimensional grating pattern displayed on the monitor, because the UV camera used here has sensitivity also in visible range. Next, UV light is irradiated on the measuring object, and images are taken with the left and right cameras.

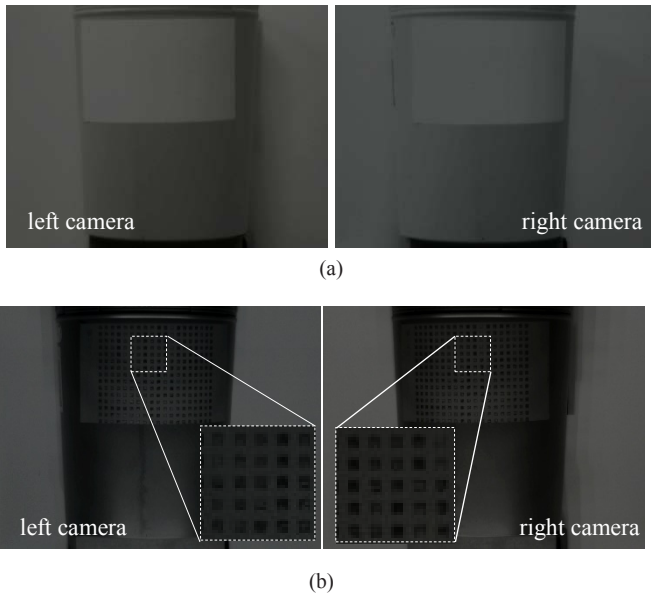


Fig. 10. Obtained UV camera images. (a) UV-camera images under fluorescent light. (b) UV-camera images under ultraviolet light.

Figure 10 shows obtained images by two UV cameras. Figure 10(a) and (b) show images under fluorescent light and under UV light, respectively. Under the UV light, we can see grating pattern emerged as black in obtained images.

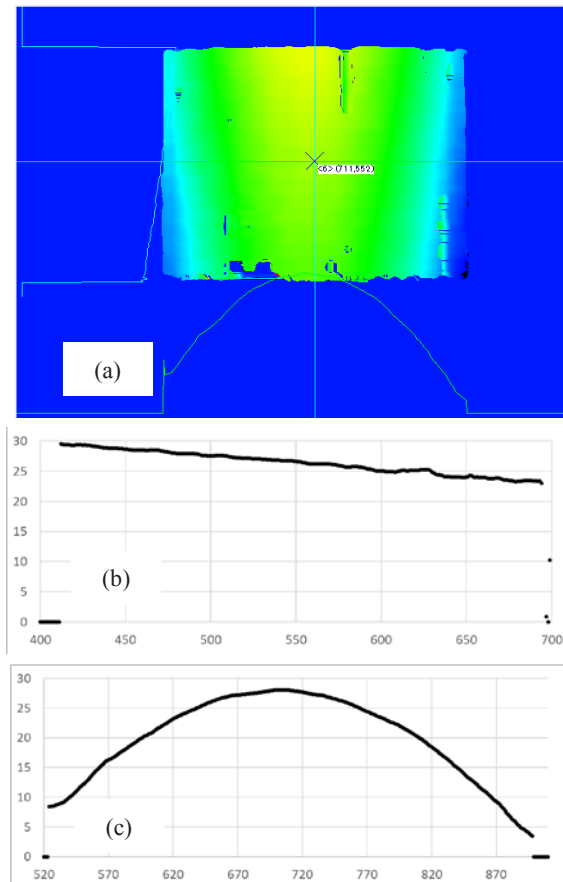


Fig. 11. Three-dimensional and sectional data obtained by UV cameras. (a) Three dimensional data. (b) Vertical sectional data at $x=711$ pixel. (c) Horizontal sectional data at $y=552$ pixel.

Figure 11(a) illustrates three-dimensional data derived from the images shown in Fig. 10(b). Figure 11(b) and (c) show vertical section data at x position is 706 pixel and horizontal section data at y position is 551 pixel, respectively.

In order to evaluate measured data shown in Fig. 11, we measured the same object by grating projection method using one VIS camera and projector shown in Fig. 5(a). Calibration was conducted in the same way as the case of UV cameras. The distance between reference plane is 30 mm. Measurement accuracy evaluated by measuring the reference surface itself multiple times was about $80 \mu\text{m}$. Three-dimensional cloud data obtained by grating projection method is shown in Fig. 12. The color of images indicate height in z -direction. Three-dimensional point cloud data is shown in Fig. 12(a). The number of points is 407,814. We generated mesh data (Fig. 12(b)) from these point cloud data to compare these two data, since the shape data obtained by the grating projection method cannot be associated with specific measurement points on the object. The mesh was generated by Delaunay triangulation based on the projection point cloud on the least square surface obtained by the original point cloud data.

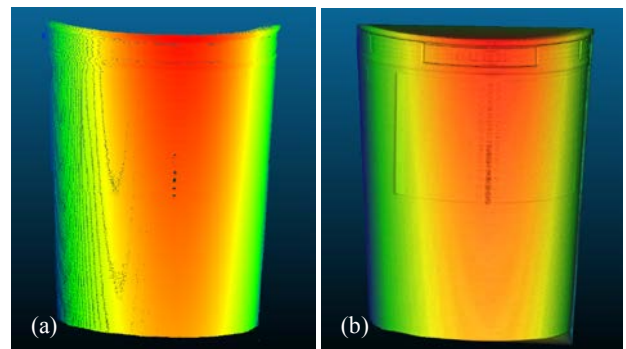


Fig. 12. Three-dimensional data obtained by grating projection method. (a) 3D point cloud data. (b) Generated mesh data.

Figure 13 shows distances from the cloud data obtained by UV cameras to the generated mesh. The number of points shown as red in Fig. 13(a) is 104,326. The same reference plane at the same place and interval are used for both calibrations for grating projection method and imparted grating pattern method using UV cameras, as can be seen in Fig. 13(a) the two data are displayed in the same coordinate system without any matching. Figure 13(b) indicates distances of the cloud data from the mesh and Fig. 13(c) shows distribution of the distances. The gray curve means an approximate Gaussian distribution. The average of the difference between the two data is $138.9 \mu\text{m}$ and the standard deviation is $412.6 \mu\text{m}$. Note that the influence of halation due to titanium oxide paintings is observed in the data measured by the grating projection method as shown in Fig. 12(b), and the difference values of this part are relatively large.

3.4. Correction of chromatic aberration

Logically, both calibration and measurement was performed in UV range. In this study, the calibration is performed in the VIS range and the measurement was performed in the UV range. Therefore, the focal length is shifted due to the axial and lateral chromatic aberration. Relatively large difference

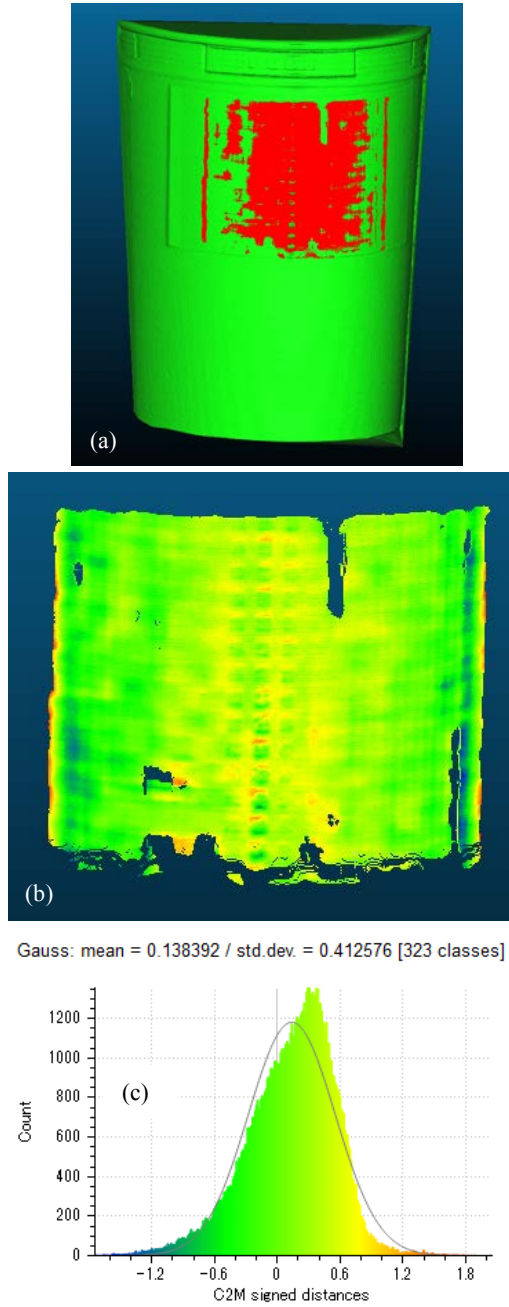


Fig. 13. Distances of the cloud data from the generated mesh. (a) Point cloud data obtained by UV cameras (red) and the generated mesh data (green). (b) Distances of cloud data from the mesh. (c) Distribution of the distances.

shown in Fig. 14 might be come from this reason. In order to correct measurement error caused by this chromatic aberration, we calculated shift value of the focal length using refractive index data on the wave length of quartz glass¹³⁾ according to the following equation.

$$\Delta f = -f\omega = -f \frac{n_2 - n_1}{n_b - 1}, \quad (1)$$

where Δf is shift value of the focal length, f is basic focal length, ω is dispersion equal to inverse of the Abbe number, n_1 and n_2 are refractive index of quartz glass for VIS and UV range, and n_b is reference refractive index value for

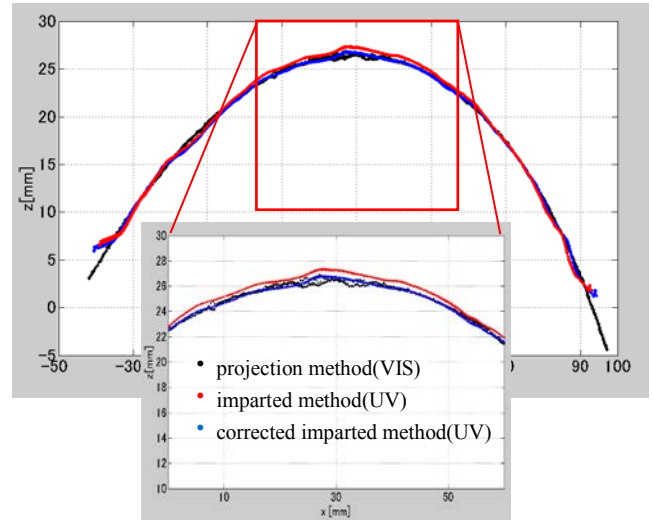


Fig. 14. Comparison of data before and after correction.

wavelength determining the basic focal length. f is 25 mm, and for n_2 and n_b , 1.46314 corresponding to the wavelength of 486.13 nm closed to the center wave length of spectral sensitivity in Fig. 2 was selected from refractive index table in Ref. 13). For n_1 1.47448 corresponding to wave length of 365.48 nm closed to the center wave length of used UV LED light was selected. The calculated focal length shift was 0.56 mm. Because we calibrated using reference plane in z -direction, the measurement results shown in Fig. 13(b) was shifted in z -direction by the shift amount of focal length, and the enlargement ratio in xy plane ($=25.56 \text{ mm}/25 \text{ mm}$) was adopted. Figure 14 shows comparison data before and after correction. Corrected data is well matched to the data of grating projection method excluding halation area. The average of the difference between the corrected data and the mesh data including halation area shown in Fig. 12 is $-42.8 \mu\text{m}$ and the standard deviation is $337.6 \mu\text{m}$. Since the variation in the measurement values of the grating projection method is about $80 \mu\text{m}$, measurement values of the imparted grating pattern method in UV range is estimated to be about $160 \mu\text{m}$.

4. Conclusion

We proposed a measurement method using ultraviolet (UV) range in which images of a grating pattern imparted on the surface of the structure are acquired by two UV cameras. This grating pattern is drawn by reflection/absorption materials in UV range, so that it is entirely seen with visible (VIS) range light as white. In this paper, we show both images in VIS/UV range of grating pattern imparted by combining UV ray reflecting/absorbing materials. And we provide result of three-dimensional measurement experiment using two UV cameras, and evaluate its effectiveness and measurement accuracy. Some conclusion remarks are summarized as below.

- A grating pattern drawn with UV reflective and absorbed material was photographed with a commercially available UV camera under UV LED light irradiation

and it was possible to obtain sufficient dynamic range. As a UV absorber, it was found that a dispersion solution of titanium oxide or zinc oxide is effective.

- It was confirmed that the grating pattern was photographed in different environments of UV intensity and that a sufficient dynamic range could be obtained for discrimination of grating pattern even in UV intensity in sunny shade on ground.
- We conducted a simple experiment to measure the object with the grating pattern and showed that the proposed method is possible. This experiment was carried out indoors under UV light, however, this method is effective outdoors or on orbit because more UV light is irradiated outdoors in clear weather and on orbit.
- In this study, because of calibration in VIS range and measurement in UV range for comparison of accuracy with the existing measurement method, errors due to chromatic aberration occurred. When correcting the focal length from the refractive index by wavelength, the measurement result by imparted grating pattern method in UV range is well matched with the measurement result by the existing grating projection method. As a matter of course, if calibration and measurement are performed in the same UV range, such correction is unnecessary.
- In this paper, for the purpose of expanding the applicability of the proposed measurement method, we extended the measurement wavelength to the UV range adding to the VIS range, but in order to discuss the interference with the thermal design, it is necessary to investigate the thermo-optical properties of the paintings.

Antenna Structure for VSOP-2 Mission, Proceedings of the 59th International Astronautical Congress, IAC-08.C2.2.5, 2008.

- 5) Tanaka, H.: Study on a Calibration Method for Shape Control Parameters of a Self-Sensing Reflector Antenna Equipped with Surface Adjustment Mechanisms, *Trans. of the JSASS*, **57**, (2014), pp. 86-92.
- 6) Morimoto, Y. and Fujigaki, M.: Automated Analysis of 3-D Shape and Surface Strain Distribution of a Moving Object Using Stereo Vision, *Optics and Lasers in Engineering*, **18** (1993), pp. 195-212.
- 7) Ri, S., Fujigaki, M., and Morimoto, Y.: Sampling Moire Method for Accurate Small Deformation Distribution Measurement, *Experimental Mechanics*, **50**, Issue 4 (2010), pp. 501-508.
- 8) Yoshikawa, T.: Improvement of Accuracy and Speed in Three-dimensional Deformation Measurement using Two-dimensional Grating Pattern, Master's Thesis, Wakayama University, 2014 (in Japanese).
- 9) Henninger, J. H.: Solar Absorptance and Thermal Emittance of Some Common Spacecraft Thermal-Control Coatings, NASA Reference Publication 1121, 1984.
- 10) http://www.artray.co.jp/download/pmanual/ARTCAM-407UV-WOM_130307_V100.pdf (Accessed April 24, 2017)
- 11) Goka, T.: Encyclopedia of Space Environment Risk, 2006, pp.29, (in Japanese).
- 12) Fukuda, J.: Development of Functional Titanium Dioxide, *Manufacturing & Technology*, **66**, (2014), pp.54-59,(in Japanese).
- 13) Quartz Glass for Optics, Shin-Etsu Quartz Products Co., Ltd., http://www.sqp.co.jp/seihin/catalog/pdf/e_3.pdf (Accessed June 23, 2017).

Acknowledgments

The author expresses appreciation for receiving titanium and zinc oxide dispersed liquid samples from TAYCA Corporation. A part of this research was supported by an A-STEP Program (No. AS262Z02432K) from JST.

References

- 1) Puig, L., Barton, A., and Rando, N.: A Review on Large Deployable Structures for Astrophysics Missions, *Acta Astronautica*, **67** (2010), pp. 12-26.
- 2) Santiago-Prowld, J., and Baier, H.: Advances in Deployable Structures and Surfaces for Large Apertures in Space, *CEAS Space Journal*, **5**, Issue 3-4 (2013), pp. 89-115.
- 3) Ishimura, K., Kii, T., Komatsu, K., Goto, K., Higuchi, K., Matsumoto, K., Ikura, S., Yoshihara, M., and Tsuchiya, M.: Shape Prediction of Large Deployable Antenna Structure on Orbit, *Trans. of JSASS Aerospace Technology Japan*, **10**, No.ists28 (2012), pp. Pc35-Pc40.
- 4) Higuchi, K., Kishimoto, N., Kawahara, K., Kimura, K., Meguro, A., Mizuno, and et. al.: Large Deployable